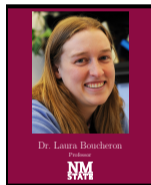
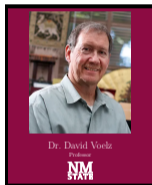
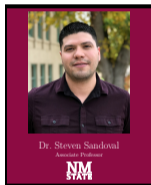
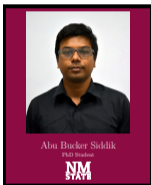


Machine Learning to Estimate Modified Zernike Coefficients for Image Point Spread Functions



Abu Bucker Siddik, **Steven Sandoval**, David Voelz, Laura E Boucheron, and Luis Varela
New Mexico State University
Klipsch School of Electrical and Computer Engineering
Las Cruces, New Mexico, U.S.A.

July 20, 2023

Outline

1 Introduction

- Atmospheric Turbulence
- Motivation and Purpose of Work

2 Background

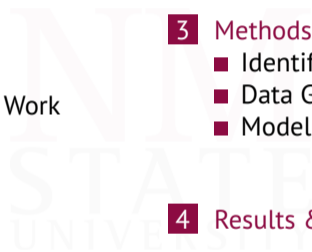
- Imaging Model
- Turbulence Model
- Wavefront Distortion Model

3 Methods

- Identify Ambiguity
- Data Generation
- Model Architecture

4 Results & Discussion

5 Acknowledgements



Atmospheric Turbulence

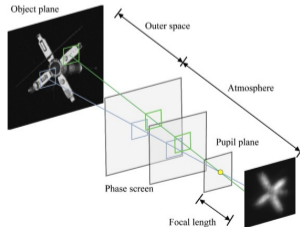
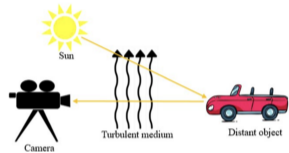
Video taken from <https://www.youtube.com/watch?v=RKKILET6aYE>

- Atmospheric turbulence usually refers to the three-dimensional, chaotic flow of air in the Earth's atmosphere.
- Atmospheric turbulence is primarily caused by the inhomogeneous refractive index in air which arises due to temperature variations and convection throughout the transmission path of the optical wave.



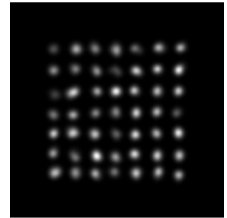
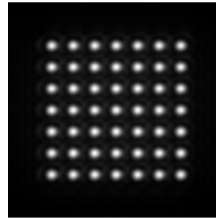
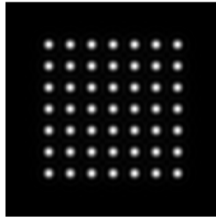
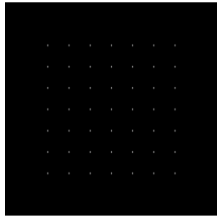
Atmospheric Turbulence

Images taken from Fazlali et al. (2022) and <https://www.sciencedirect.com/science/article/abs/pii/S0030402620300115>



- The extent of wave degradation resulting from atmospheric turbulence depends on the intensity of fluctuations in the refractive index of air.
- Estimation/correction of atmospheric turbulence and its effects on light has many applications. For example, long-distance aiming of laser (target designation, energy focusing, and secure communications) and long-range terrestrial observations using visible and infrared imaging systems are susceptible to degradations from atmospheric turbulence.

Isoplanatic Turbulence and Anisoplanatic Turbulence

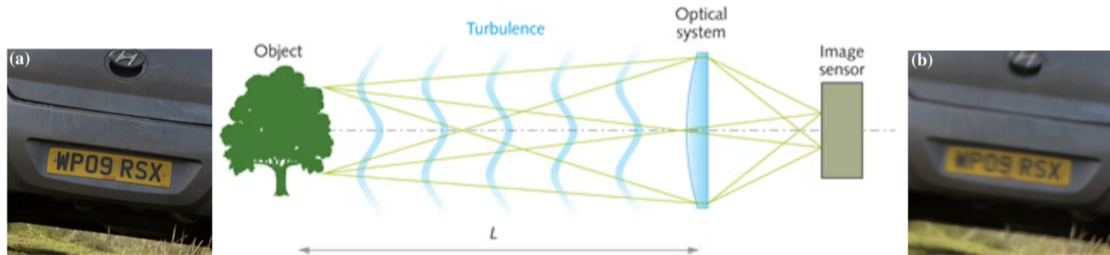


- If the degradation caused by the turbulence is uniform across the field of view of the imaging system, the turbulence can be considered isoplanatic.
- Anisoplanatic turbulence, on the other hand, introduces varying degrees of degradation throughout the field of view, making it more difficult to correct the turbulence-degraded images as opposed to isoplanatic turbulence.

Motivation

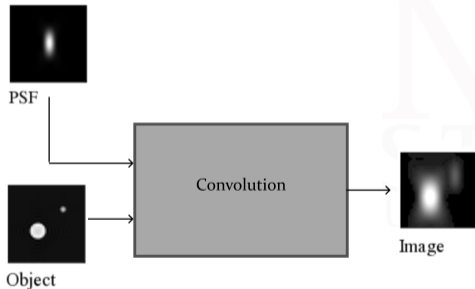
Images taken from Fazlali et al. (2022) and <https://www.laserfocusworld.com/>

- In long-range imaging, the quality of an image is degraded by atmospheric turbulence.
- Reflected light from a distant object passes several turbulent layers to reach the camera.
- Geometric distortion and blurring in the image.



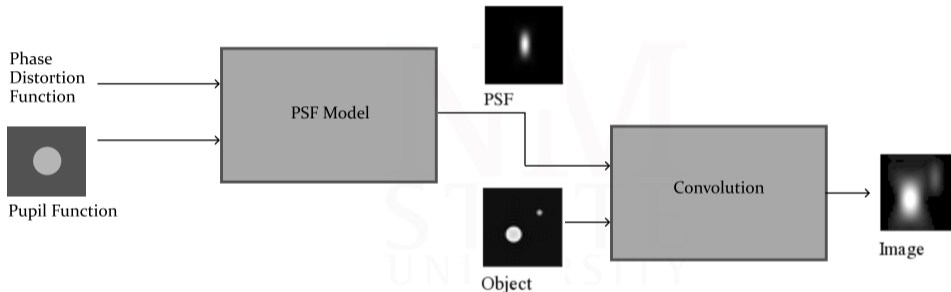
Motivation

Li et al. (2018) Figure taken from Wikipedia contributors (2023)



- The point spread function (PSF) refers to the impulse response of an imaging system.
- The degradation of an image caused by turbulence can be described by the point spread function.
- Under anisoplanatic imaging conditions, the degradation is modeled by a spatially varying PSF across the pixels.
- Estimating the PSF from a degraded image is the initial step for correcting image distortion.

Motivation

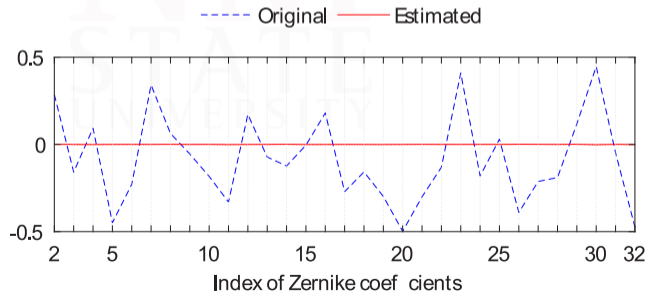
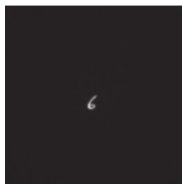


- The point spread function (PSF) can be modeled by a Pupil Function and a Phase Distortion Function

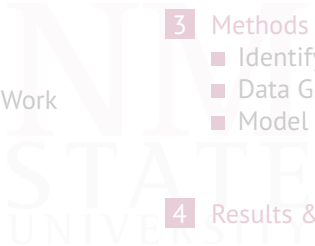
Purpose of Work

Jin et al. (2018); Paine and Fienup (2018); Zhang et al. (2019); Tian et al. (2019); Lu et al. (2022) Figures taken from Nishizaki et al. (2019)

- A common way to parameterize the distortions is by modeling the phase distortions of monochromatic waves with Zernike coefficients.
- Unfortunately, other researchers have had little success trying to directly predict Zernike coefficients from intensity images alone.

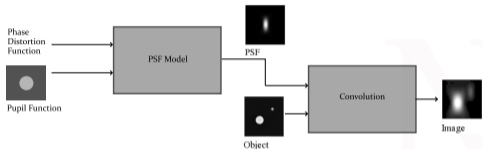


Outline

- 
- 1 Introduction
 - Atmospheric Turbulence
 - Motivation and Purpose of Work
 - 2 Background
 - Imaging Model
 - Turbulence Model
 - Wavefront Distortion Model
 - 3 Methods
 - Identify Ambiguity
 - Data Generation
 - Model Architecture
 - 4 Results & Discussion
 - 5 Acknowledgements

Imaging Model

Lu et al. (2022)



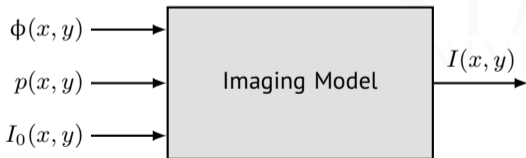
- Incoherent imaging of an object can be modeled using a linear, space-invariant forward model

$$I(x, y) = h(x, y) * I_0(x, y)$$

- $I(x, y)$ is intensity image of a source object $I_0(x, y)$.
- PSF $h(x, y)$ can be expressed as

$$h(x, y) \propto |\mathcal{F}\{p(x, y)e^{j\phi(x, y)}\}|^2,$$

where $p(x, y)$ is the pupil function, and $\phi(x, y)$ is the wavefront phase distortion.

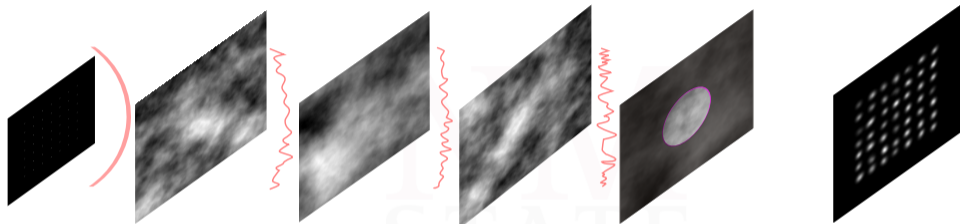


Imaging Model



- In a vacuum, light originating at the source spherically propagates outward until it reaches the entrance pupil of the physical aperture.
- Assuming a long-range imaging scenario, the curvature of the wavefront arriving at the aperture is roughly flat.
- The resulting image has no distortion due to turbulence, rather the image is diffraction-limited by the physical system.

Imaging Model



- The propagation of light through a medium such as the atmosphere introduces wavefront aberrations at the aperture plane that further degrade the images.
- In this case, the PSF captures the combined effects of both the diffraction-limited imaging system and the distortion due to turbulence.
- Therefore, estimation of the combined system and medium PSF can potentially quantify the aberrations so that image correction can be performed.

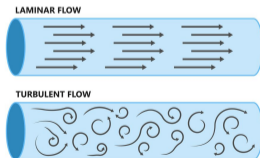
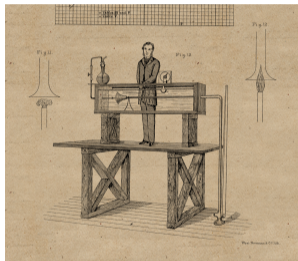
Imaging Model



- To simplify our initial investigation, we investigate the effects of a single phase screen.

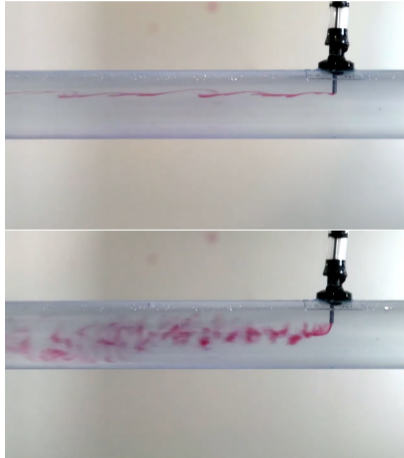
Turbulence

Jousef Murad (2023)



- Osborne Reynolds (1842-1912) was a pioneer in the study of fluid dynamics,
- In 1883, he performed a simple but elegant experiment to investigate the flow of fluids through tubes.
- Reynolds passed water through a pipe at different flow velocities and introduced dye into the tubes to visualize fluid flow behavior.

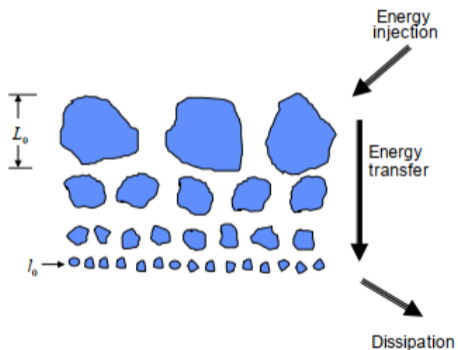
Jousef Murad (2023), Video taken from <https://www.youtube.com/watch?v=vhDaCZZ0Sc4>



- Reynolds showed most effectively that the characteristics of the flow vary with the flow velocity, and demonstrated the features of laminar and turbulent flow.
- Moreover, the transition point between the two types of flow could be predicted by one simple number (the Reynolds number).
- The Reynolds number remains the standard mathematical framework to study laminar & turbulent fluid systems.

Modeling Atmospheric Turbulence: Kolmogorov's Theory

Figures taken from



- Kolmogorov's theory offers a mathematical expression for the statistics of the atmosphere's refractive index variations.
- Wind breaks down large-scale inhomogeneities into smaller ones and the turbulent air motion gives rise to eddies with varying sizes and speeds.
- Kolmogorov considers the span of turbulence flows from macroscale structure to microscale structure.

Modeling Atmospheric Turbulence: Kolmogorov's Theory

Figures taken from

■ Assumptions:

- As the characteristic diameter of the eddy decreases, the characteristic orbital velocity of the eddy decreases.
- Small-scale eddies are statistically homogeneous and isotropic.
- Separation of scales is high or infinity.
- At the macroscale, energy is supplied to turbulence flow from wind shear or convection.

■ Kolmogorov's view:

- Energy transfers from large-scale eddies to small-scale eddies.
- At the microscale (l_0), energy is dissipated as heat due to viscosity.
- For inertial subrange, the spectral power spectral density $\Phi_n(\vec{\mathcal{K}})$ of the refractive index of the atmosphere (n)

$$\Phi_n(\vec{\mathcal{K}}) = 0.033C_n^2\mathcal{K}^{-11/3},$$

where $\vec{\mathcal{K}}$ is the spatial wave number vector and C_n^2 is the structure constant of refractive index fluctuations.

Wavefront Distortion Representation

Lakshminarayanan and Fleck (2011)

- The wavefront phase distortion can be represented by a linear superposition of Zernike polynomials

$$\phi(x, y) = \sum_{n,m} a_{nm} Z_n^m(x, y)$$

$$\phi(x, y) = \sum_q a_q Z_q(x, y)$$

- Zernike polynomials form a set of orthogonal functions defined over the unit circle.

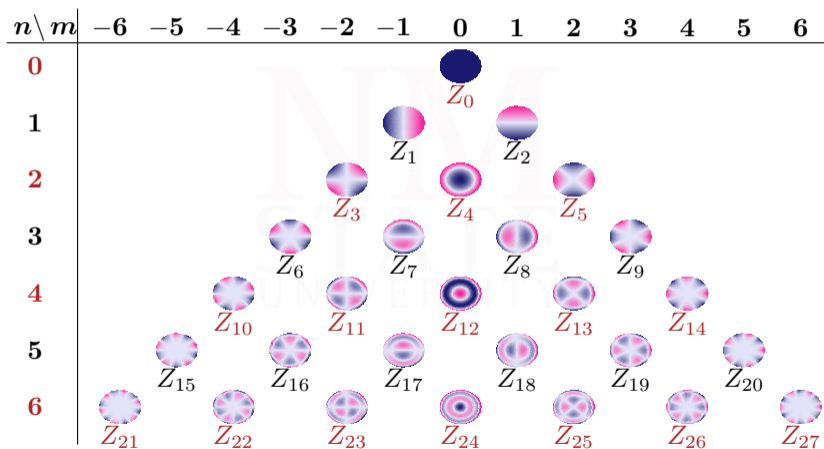
$$Z_n^m(\rho, \varphi) = \begin{cases} R_n^{|m|}(\rho) \cos(m\varphi), & \text{if } m \geq 0 \\ R_n^{|m|}(\rho) \sin(m\varphi), & \text{if } m < 0 \end{cases}$$

- Single indexing: $q = (n(n+2) + m)/2$

$$\text{Wavefront} = a_0 \left(\text{circle} \right) + a_1 \left(\text{circle} \right) + a_2 \left(\text{circle} \right) + a_3 \left(\text{circle} \right) + a_4 \left(\text{circle} \right) + a_5 \left(\text{circle} \right) + \dots$$

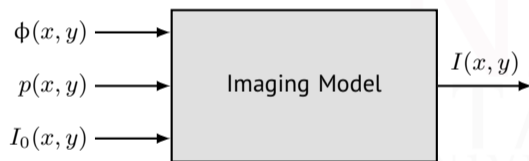
Zernike Polynomials

Lakshminarayanan and Fleck (2011)



Relationship between Zernike Coefficients and Intensity Image

- Wavefront phase distortion with single-indexed Zernike polynomials

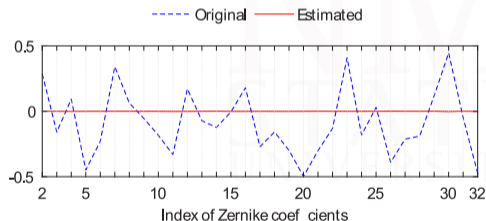
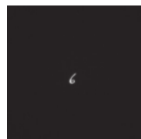


$$\phi(x, y) = \sum_q a_q Z_q(x, y)$$

- Already observed that intensity image $I(x, y) = h(x, y) * I_0(x, y)$ and PSF $h(x, y) \propto |\mathcal{F}\{p(x, y)e^{j\phi(x, y)}\}|^2$
- Zernike coefficients a_q correspond to a particular $I(x, y)$ and can be used to parameterize the associated PSF of an aberrated imaging system.

Ambiguity for Predicting the Zernike Coefficients from Intensity Images

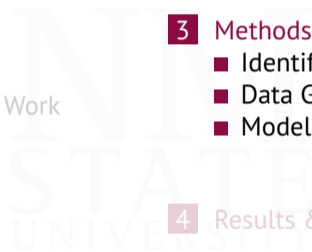
Jin et al. (2018); Paine and Fienup (2018); Zhang et al. (2019); Tian et al. (2019); Lu et al. (2022) Figures taken from Nishizaki et al. (2019)



- Utilize deep learning (DL) models to predict Zernike coefficients from intensity images
- Ambiguity involving the prediction of Zernike coefficients
- Some Zernike polynomials Z_q generate the same PSF intensity image for oppositely-signed Zernike coefficients

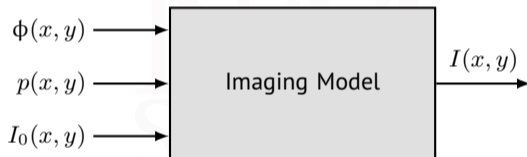
Outline

- 1 Introduction
 - Atmospheric Turbulence
 - Motivation and Purpose of Work
- 2 Background
 - Imaging Model
 - Turbulence Model
 - Wavefront Distortion Model
- 3 Methods
 - Identify Ambiguity
 - Data Generation
 - Model Architecture
- 4 Results & Discussion
- 5 Acknowledgements



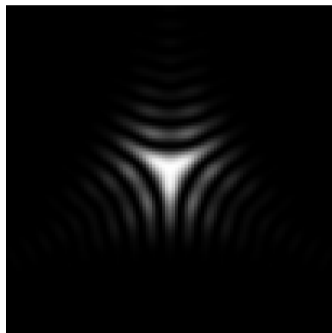
Ambiguity

Bracewell and Bracewell (1986)

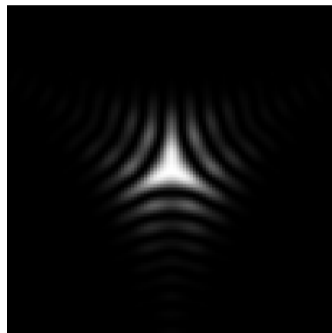


- Identify the Zernike polynomials which are susceptible to ambiguity
- Use symmetry properties of the Fourier transform to mathematically prove that angularly even polynomials introduce ambiguity

PSF intensity images of a point object with Z_6



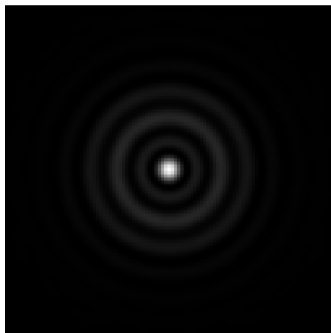
(a)



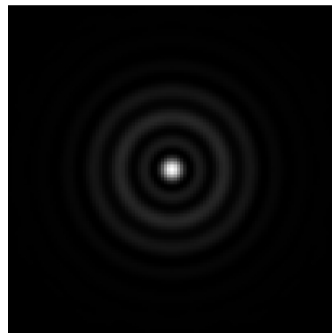
(b)

Figure: The PSF intensity images of a point object with: (a) Zernike coefficient value $+5$ for Z_6
(b) Zernike coefficient value -5 for Z_6

PSF intensity images of a point object with Z_{12}



(a)



(b)

Figure: The PSF intensity images of a point object with: (a) Zernike coefficient value +5 for Z_{12} (b) Zernike coefficient value -5 for Z_{12}

Identify Ambiguity

- Express $h(x, y)$ in terms of the Fourier transform as

$$h(x, y) \propto \mathcal{F} \left\{ p(x, y) e^{j\phi(x, y)} \right\} \mathcal{F}^* \left\{ p(x, y) e^{j\phi(x, y)} \right\},$$

- Express $p(x, y)$ and $\phi(x, y)$ in terms of real/imaginary and even/odd parts as

$$p(x, y) = p_{\text{re}}(x, y) + \cancel{p_{\text{ro}}(x, y)} + \cancel{j p_{\text{ie}}(x, y)} + \cancel{j p_{\text{io}}(x, y)}$$

and

$$\phi(x, y) = \phi_{\text{re}}(x, y) + \phi_{\text{ro}}(x, y) + \cancel{j \phi_{\text{ie}}(x, y)} + \cancel{j \phi_{\text{io}}(x, y)}$$

Identify Ambiguity

- An angularly even Zernike polynomial $Z_{ae}(x, y)$ produces a real even symmetric $\phi(x, y)$.

$$\begin{aligned}\mathcal{F}\left\{p(x, y)e^{j\phi(x, y)}\right\} &= \mathcal{F}\left\{p_{re}(x, y)e^{j\phi_{re}(x, y)}\right\} \\ &= \mathcal{F}\left\{p_{re}(x, y)\cos\phi_{re}(x, y) + jp_{re}(x, y)\sin\phi_{re}(x, y)\right\}\end{aligned}$$

- For Zernike coefficient $\pm a$, we have $\phi_{re}(x, y) = \pm aZ_{ae}(x, y)$ and

$$\begin{aligned}\mathcal{F}\left\{p(x, y)e^{\pm jaZ_{ae}(x, y)}\right\} &= \mathcal{F}\left\{p_{re}(x, y)\cos[\pm aZ_{ae}(x, y)] + jp_{re}(x, y)\sin[\pm aZ_{ae}(x, y)]\right\} \\ &= \mathcal{F}\left\{p_{re}(x, y)\cos[aZ_{ae}(x, y)] \pm jp_{re}(x, y)\sin[aZ_{ae}(x, y)]\right\} \\ &= A(x, y) \pm jB(x, y)\end{aligned}$$

- $A(x, y) \stackrel{\mathcal{F}}{\leftrightarrow} p_{re}(x, y)\cos[aZ_{ae}(x, y)]$ is real even and $jB(x, y) \stackrel{\mathcal{F}}{\leftrightarrow} jp_{re}(x, y)\sin[aZ_{ae}(x, y)]$ is imaginary even. This leads to

$$h(x, y) \propto \left|\mathcal{F}\left\{p_{re}(x, y)e^{j\phi_{re}(x, y)}\right\}\right|^2 = A^2(x, y) + B^2(x, y).$$

Identify Ambiguity

- An angularly odd Zernike polynomial $Z_{ao}(x, y)$ produces a real odd symmetric $\phi(x, y)$.

$$\begin{aligned}\mathcal{F}\left\{p(x, y)e^{j\phi(x, y)}\right\} &= \mathcal{F}\left\{p_{re}(x, y)e^{j\phi_{ro}(x, y)}\right\} \\ &= \mathcal{F}\left\{p_{re}(x, y)\cos\phi_{ro}(x, y) + jp_{re}(x, y)\sin\phi_{ro}(x, y)\right\}\end{aligned}$$

- For Zernike coefficient $\pm a$, we have $\phi_{ro}(x, y) = \pm aZ_{ao}(x, y)$ and

$$\begin{aligned}\mathcal{F}\left\{p(x, y)e^{\pm jaZ_{ao}(x, y)}\right\} &= \mathcal{F}\left\{p_{re}(x, y)\cos[\pm aZ_{ao}(x, y)] + jp_{re}(x, y)\sin[\pm aZ_{ao}(x, y)]\right\} \\ &= \mathcal{F}\left\{p_{re}(x, y)\cos[aZ_{ao}(x, y)] \pm jp_{re}(x, y)\sin[aZ_{ao}(x, y)]\right\} \\ &= C(x, y) \pm D(x, y)\end{aligned}$$

- $C(x, y) \xleftrightarrow{\mathcal{F}} p_{re}(x, y)\cos[aZ_{ao}(x, y)]$ is a real even and $D(x, y) \xleftrightarrow{\mathcal{F}} jp_{re}(x, y)\sin[aZ_{ao}(x, y)]$ is real odd. This leads to

$$h(x, y) \propto \left|\mathcal{F}\left\{p_{re}(x, y)e^{j\phi_{ro}(x, y)}\right\}\right|^2 = [C(x, y) \pm D(x, y)]^2.$$

Ambiguity

- Consider the prediction of the absolute value of the associated Zernike coefficients for angularly even polynomials
- Refer signless coefficients for angularly even polynomials and signed coefficients for angularly odd polynomials as the *modified Zernike coefficients*
- Use a deep neural network to predict the modified coefficients directly from PSF intensity images

Data Generation

Underwood and Voelz (2013); Zhan et al. (2019); Schmidt (2010); Wilcox (2023); Jin et al. (2018); Paine and Fienup (2018); Delabie et al. (2014); Noll (1976)

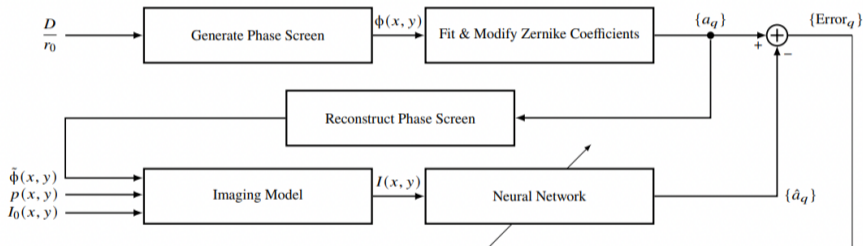


Figure: Block diagram of the proposed training methodology.

Data Generation

Cohen et al. (2017)



Figure: PSF intensity image of an extended source object: (a) source object (b) intensity image for $\frac{D}{r_0} = 10$

Dataset Generation

Paine and Fienup (2018)

- We consider four different scenarios at nine atmospheric turbulence strengths $D/r_0 = 2, 3, \dots, 10$
 - Point source object with zero noise
 - Extended source objects with zero noise
 - Extended source objects with low noise: Poisson noise with peak photon levels of 4000 and read out noise with zero mean, standard deviation 10
 - Extended source objects with high noise: Poisson noise with peak photon levels of 15000 and read out noise with zero mean, standard deviation 100
- We use one point source object and 6000 different extended source objects (5000/500/500 for training/validation/testing purposes)

Model Architecture

Hu et al. (2020); Krizhevsky et al. (2012); Bezanson et al. (2012); Innes (2018); Hu et al. (2020); Kingma and Ba (2014)

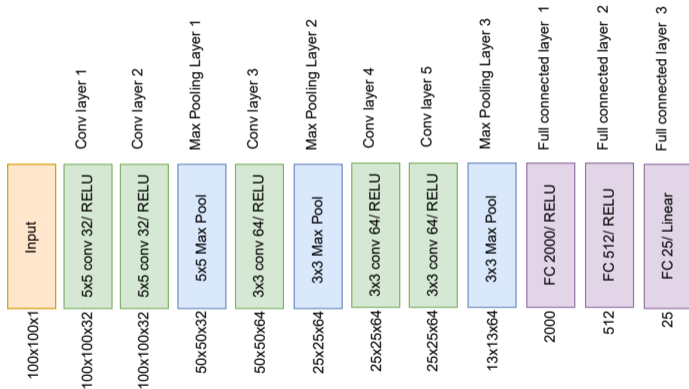
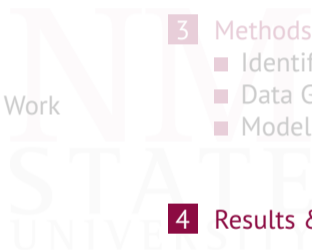


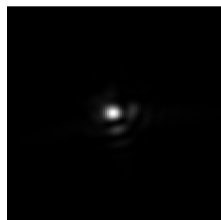
Figure: The neural network architecture used in the proposed estimation.

Outline

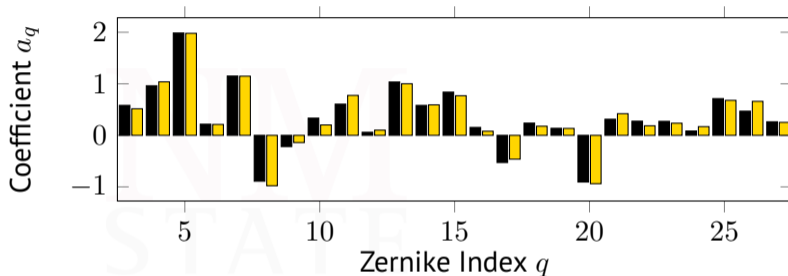
- 1 Introduction
 - Atmospheric Turbulence
 - Motivation and Purpose of Work
- 2 Background
 - Imaging Model
 - Turbulence Model
 - Wavefront Distortion Model
- 3 Methods
 - Identify Ambiguity
 - Data Generation
 - Model Architecture
- 4 Results & Discussion
- 5 Acknowledgements



Results & Discussion



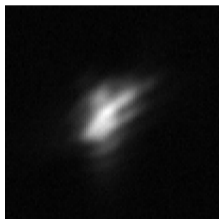
(a)



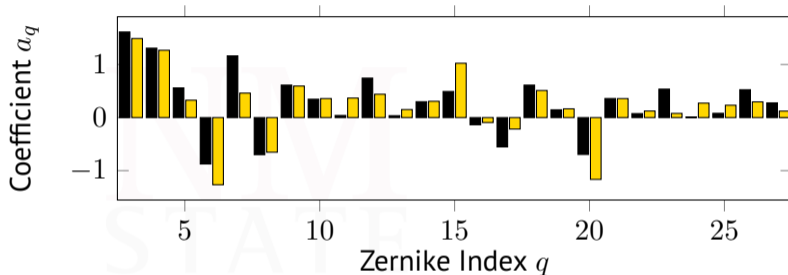
(b)

Figure: Demonstration of the proposed estimation for a point source object with zero noise. (a) intensity image for $D/r_0 = 5$ (b) the actual (■) and predicted (■) Zernike coefficients corresponding to the intensity image in (a).

Results & Discussion



(a)



(b)

Figure: Demonstration of the proposed estimation for an extended source object with high noise. (a) intensity image for $D/r_0 = 5$ (b) the actual (■) and predicted (■) Zernike coefficients corresponding to the intensity image in (a).

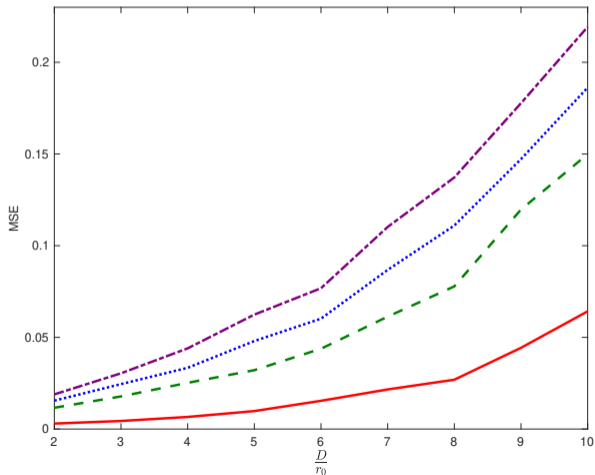
Results & Discussion

Table: Average MSE for the four scenarios.

Scenario	Average MSE	Description
1	0.0218	Point Source Object
2	0.0599	Extended Source Objects
3	0.0792	Extended Source Objects with Low Noise
4	0.0974	Extended Source Objects with High Noise

- MSE of 0.5673 for scenario 1 with the signed Zernike coefficients for all polynomials

Results & Discussion



The MSE as a function of D/r_0 for (—) a point source object with no noise, (---) extended source objects with no noise, (·····) extended source objects with low noise, and (-·-·-) extended source objects with high noise

Results & Discussion

- Data for the learning model was created with an image simulation of a point object and simple extended objects for a range of turbulence and detection noise levels.
- The modified set of Zernike Coefficients was shown to be sufficient for specifying the intensity PSF.
- As expected, the results show that the point source object with no noise produces the lowest average MSE whereas the extended source objects with high noise give the largest MSE.
- The prediction MSE for the learning model shows that it is possible to recover a useful set of modified Zernike coefficients from an extended object intensity image subject to noise and turbulence.
- In all cases, the MSE increases in a predictable way with turbulence strength (D/r_0).

More Information



Deep learning estimation of modified Zernike coefficients and recovery of point spread functions in turbulence

ABU BUCKER SIDDIK,^{*} STEVEN SANDOVAL, DAVID VOELZ, LAURA E. BOUCHERON, AND LUIS VARELA

Kilgus School of Electrical and Computer Engineering, New Mexico State University, Las Cruces, NM 88002, USA
^{*}sid01@nmsu.edu

Abstract: Recovering the turbulence-degraded point spread function from a single intensity image is important for a variety of imaging applications. Here, a deep learning model based on a convolutional neural network is applied to intensity images to predict a modified set of Zernike polynomial coefficients corresponding to wavefront aberrations in the pupil due to turbulence. The modified set assigns an absolute value to coefficients of even radial orders due to a sign ambiguity associated with this problem and is shown to be sufficient for specifying the intensity point spread function. Simulated image data of a point object and simple extended objects over a range of turbulence and detection noise levels are created for the learning model. The MSE results for the learning model show that the best prediction is found when observing a point object, but it is possible to recover a useful set of modified Zernike coefficients from an extended object image that is subject to detection noise and turbulence.

© 2023 Optica Publishing Group under the terms of the Optica Open Access Publishing Agreement

1. Introduction

The point spread function (PSF) refers to the impulse response of an imaging system [1]. When the PSF is known, it can be used for the correction of blur and other artifacts in images that are due to the system's response. For example, in a space-invariant imaging situation, a PSF correction might be applied in a deconvolution step. Additionally, the propagation of light through a medium such as the atmosphere introduces wavefront aberrations at the aperture plane that further degrade the images. Therefore, the estimation of the combined system and medium PSF can potentially quantify the aberrations so that image correction can be performed.

1.1. Imaging model

Incoherent imaging of an object can be modeled using a linear space-invariant forward model

$$I(x, y) = h(x, y) * I_0(x, y), \quad (1)$$

where $I(x, y)$ is the intensity image of a source object $I_0(x, y)$, $*$ is the convolution operator, and $h(x, y)$ is the intensity PSF given by

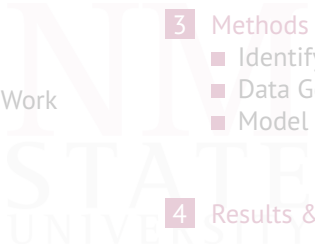
$$h(x, y) = |\mathcal{F}[p(x, y)e^{i\phi(x, y)}]|^2, \quad (2)$$

where \mathcal{F} is the Fourier transform, $|\cdot|$ is the modulus operator, $p(x, y)$ is the pupil function, and $\phi(x, y)$ is the wavefront phase distortion applied at the pupil plane [2].

1.2. Representing wavefront distortions

Although the PSF can be parameterized in various ways, to leverage results from disciplines such as adaptive optics, we consider the wavefront distortion $\phi(x, y)$ related to the PSF through Eq. (2).

Outline

- 
- 1 Introduction
 - Atmospheric Turbulence
 - Motivation and Purpose of Work
 - 2 Background
 - Imaging Model
 - Turbulence Model
 - Wavefront Distortion Model
 - 3 Methods
 - Identify Ambiguity
 - Data Generation
 - Model Architecture
 - 4 Results & Discussion
 - 5 Acknowledgements

Acknowledgements

This work was funded by the Office of Naval Research (N00014-21-1-2430).



References I

- J. Bezanson, S. Karpinski, V. B. Shah, and A. Edelman. Julia: A fast dynamic language for technical computing. *arXiv preprint arXiv:1209.5145*, 2012.
- R. N. Bracewell and R. N. Bracewell. *The Fourier transform and its applications*, volume 31999. McGraw-Hill New York, 1986.
- G. Cohen, S. Afshar, J. Tapson, and A. Van Schaik. Emnist: Extending mnist to handwritten letters. In *2017 international joint conference on neural networks (IJCNN)*, pages 2921–2926. IEEE, 2017.
- T. Delabie, J. D. Schutter, and B. Vandenbussche. An accurate and efficient gaussian fit centroiding algorithm for star trackers. *The Journal of the Astronautical Sciences*, 61(1):60–84, 2014.
- H. Fazlali, S. Shirani, M. Bradford, and T. Kirubarajan. Atmospheric turbulence removal in long-range imaging using a data-driven-based approach. *International Journal of Computer Vision*, 130(4):1031–1049, 2022.
- S. Hu, L. Hu, B. Zhang, W. Gong, and K. Si. Simplifying the detection of optical distortions by machine learning. *Journal of Innovative Optical Health Sciences*, 13(03):2040001, 2020.
- M. Innes. Flux: Elegant machine learning with julia. *Journal of Open Source Software*, 3(25):602, 2018.
- Y. Jin, Y. Zhang, L. Hu, H. Huang, Q. Xu, X. Zhu, L. Huang, Y. Zheng, H.-L. Shen, W. Gong, et al. Machine learning guided rapid focusing with sensor-less aberration corrections. *Optics express*, 26(23):30162–30171, 2018.
- Jousef Murad. The reynolds number. <https://www.jousefmurad.com/fluid-mechanics/the-reynolds-number/>, 2023. [Online; accessed 7-July-2023].
- D. P. Kingma and J. Ba. Adam: A method for stochastic optimization. *arXiv preprint arXiv:1412.6980*, 2014.
- A. Krizhevsky, I. Sutskever, and G. E. Hinton. Imagenet classification with deep convolutional neural networks. *Advances in neural information processing systems*, 25, 2012.
- V. Lakshminarayanan and A. Fleck. Zernike polynomials: a guide. *Journal of Modern Optics*, 58(7):545–561, 2011.
- J. Li, F. Xue, F. Qu, Y.-P. Ho, and T. Blu. On-the-fly estimation of a microscopy point spread function. *Optics express*, 26(20):26120–26133, 2018.

References II

- C. Lu, Q. Tian, L. Zhu, R. Gao, H. Yao, F. Tian, Q. Zhang, and X. Xin. Mitigating the ambiguity problem in the cnn-based wavefront correction. *Optics Letters*, 47(13):3251–3254, 2022.
- Y. Nishizaki, M. Valdivia, R. Horisaki, K. Kitaguchi, M. Saito, J. Tanida, and E. Vera. Deep learning wavefront sensing. *Optics express*, 27(1):240–251, 2019.
- R. J. Noll. Zernike polynomials and atmospheric turbulence. *JOsA*, 66(3):207–211, 1976.
- S. W. Paine and J. R. Fienup. Machine learning for improved image-based wavefront sensing. *Optics letters*, 43(6):1235–1238, 2018.
- J. Schmidt. Numerical simulation of optical wave propagation with examples in matlab, vol. *PM199 (SPIE, 2010)*, 2010.
- Q. Tian, C. Lu, B. Liu, L. Zhu, X. Pan, Q. Zhang, L. Yang, F. Tian, and X. Xin. Dnn-based aberration correction in a wavefront sensorless adaptive optics system. *Optics express*, 27(8):10765–10776, 2019.
- T. A. Underwood and D. G. Voelz. Wave optics approach for incoherent imaging simulation through distributed turbulence. In *Unconventional Imaging and Wavefront Sensing 2013*, volume 8877, pages 112–119. SPIE, 2013.
- Wikipedia contributors. Point spread function – Wikipedia, the free encyclopedia. https://en.wikipedia.org/w/index.php?title=Point_spread_function&oldid=1138243509, 2023. [Online; accessed 20-February-2023].
- C. Wilcox. Zernike polynomial coefficients for a given wavefront using matrix inversion in matlab. <https://www.mathworks.com/matlabcentral/fileexchange/27072-zernike-polynomial-coefficients-for-a-given-wavefront-using-matrix-inversion-in-matlab>, 2023. MATLAB Central File Exchange [retrieved February 6, 2023].
- H. Zhan, E. Wijerathna, and D. Voelz. Wave optics simulation studies of the fried parameter for weak to strong atmospheric turbulent fluctuations. In *Propagation Through and Characterization of Atmospheric and Oceanic Phenomena*, pages PM1C–3. Optica Publishing Group, 2019.
- Y. Zhang, C. Wu, Y. Song, K. Si, Y. Zheng, L. Hu, J. Chen, L. Tang, and W. Gong. Machine learning based adaptive optics for doughnut-shaped beam. *Optics Express*, 27(12):16871–16881, 2019.